



Statistical Modelling of Solar Photocatalytic Biodegradability of Seawater Using Combined Photocatalysts

Nayeemuddin Mohammed¹ ·
Puganeshwary Palaniandy¹ · Feroz Shaik² ·
Hiren Mewada²

Received: 7 May 2022 / Accepted: 17 August 2023 / Published online: 1 September 2023
© The Institution of Engineers (India) 2023

Abstract Seawater contamination is a major environmental issue worldwide. Numerous technologies and different approaches have been used to filter out the contaminants that are found in saltwater. In this study, using a mixture of photo catalysts, TiO₂ and ZnO, a batch reactor was used to conduct an experimental research on the solar photocatalytic degradation of contaminants found in seawater. The impacts of catalyst dosage, pH and reaction duration were evaluated based on percentage elimination efficiencies of total organic carbon (TOC), chemical oxygen demand (COD), biological oxygen demand (BOD) and biodegradability (BOD/COD). The (RSM, design expert) central composite design (CCD) was used to create a statistical model. Artificial neural network optimization analysis was also performed, and its predicted values were compared to experimental and RSM anticipated values. Based on the results of the studies, the highest percentage removal efficiencies of TOC, COD, BOD, and BOD/COD were determined to be 56.9%, 73.5%, 23.0%, and 0.053, respectively. Whereas, with both statistics model found to be 51.6%, 56.8%; 71.1%, 73.5%; 22.6%, 23.5% and 0.0506, 0.0512; respectively at a photo catalyst dosage of 4 g/L, the reaction time 180 min and pH 7.5. Both

the statistical model predicted values were well closely linked with the experimental values. The RSM-CCD modeling $R^2=0.8479$ was found to be inferior than the $R^2=0.999$ average of the projected values of the ANN model.

Keywords Solar photo catalysis · Photo catalyst · Seawater · Titanium dioxide (TiO₂) · Zinc oxide (ZnO) · Biodegradability · RSM-CCD · ANN-LM

Introduction

The requirement of clean and pure water has been extremely essential on a day-to-day basis. Due to increase in the population growth all over the world, the demand or the supply of drinkable water is a major issue. Seawater is one of the largest sources to generate fresh water, but in addition to salt, it also contains a range of organic, inorganic, and biological contaminants. Prior to feeding saltwater into the primary desalination process, these pollutants must be removed. A lot of conventional methods are being used to clean up the contaminants in seawater. But recently, sophisticated oxidation techniques have been used to remediate the contaminants in the saline water. [1–8].

Heterogeneous photo catalysis is commonly used to remediate contaminants in water streams, especially salt water. This process involves a semiconductor like TiO₂, SnO₂, ZnO, PbO, etc., as a photo catalyst and is irradiated by the artificial or natural light source. During irradiation, photon energy is absorbed by the electrons in the valence band, which are further stimulated in the conduction band [9]. The formation of positive holes (h⁺) in the valence band results from the motion of electrons between the valence band and the conduction band. These positive holes interact with the water molecules to create hydroxyl radicals, and the oxygen

✉ Nayeemuddin Mohammed
mnayeemuddin@student.usm.my

Puganeshwary Palaniandy
cepuganeshwary@usm.my

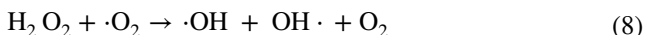
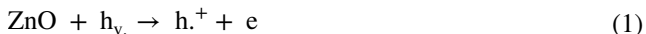
Feroz Shaik
ferozs2005@gamil.com; fshaik@pmu.edu.sa

Hiren Mewada
hmewada@pmu.edu.sa

¹ School of Civil Engineering, Universiti Sains Malaysia, Penang, Malaysia

² Prince Mohammad Bin Fahd University, Al Khobar, Kingdom of Saudi Arabia

consumes the electrons that were driven to the conduction band to create super oxide [10]. The highly oxidative reagents generated hydroxyl radicals and super oxides may both rapidly oxidize the contaminants present in the ocean [11]. Equations 1 to 9 illustrate the heterogeneous photo catalysis mechanism process [1].



Numerous studies have used the solar photocatalytic degradation mechanism to remove contaminants found in saltwater. To explore the light degradation of contaminants in salt water, a batch re-circulation reactor system was used. A combination of TiO₂ photo catalyst with polyamide was used and the effectiveness of photo catalytic degradation was assessed by measuring several parameters such as TOC, total dissolved solids (TDS), COD and total inorganic carbon (TIC). The significant parameter drop was seen during

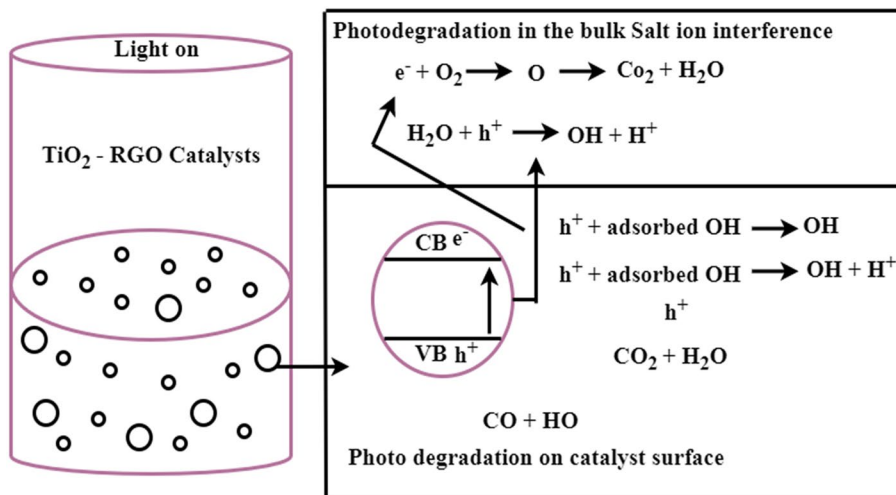
Table 1 Preliminary parameters for a seawater sample

Initial parameter	Val
COD “mg/L”	111
BOD “mg/L”	1.75
TOC “mg/L”	2.74
pH	8.655
Biodegradability “BOD/ COD”	0.016

the solar photo degradation phase [2]. In the solar photo catalytic degradation process employing Yb-TiO₂-rGO photo catalysts, a substantial decrease of phenol contained in saline water was noticed. The photo catalyst was grafted with ethylene glycol to resist the adsorption of salt ions. Figure 1 shows the schematic diagram of the photo catalytic process using Yb-TiO₂-rGO photo catalyst [3].

An artificial light source (UV lamp) was utilized with an immobilized photo catalyst (TiO₂) in plug flow reactors. The photo catalytic performance was evaluated by studying the degradation of model organic compounds, benzoic acid. Significant benzoic acid degradation was seen in plug flow reactors of various diameters [4]. The process of photo catalysis has been employed and proven a plausible technology for the decontamination of phenolic waste waters under different conditions. Photo catalysis was performed in batch reactor with recycle stream and able to achieve complete mineralization of phenol [5]. The solar photocatalytic destruction of diesel pollutants found in saltwater was studied by Qiuyi Ji et al. [6]. To evaluate the effectiveness of photo catalytic degradation of diesel pollutants present in seawater, the initial concentration of diesel pollutants, pH, catalyst ratio, and dose were changed. It was shown that 78.7% degradation of diesel pollutants during this visible photo catalytic degradation process [6]. The oil produced water consisting of organic and inorganic pollutants was subjected to Nano solar photo catalysis. Experiments were performed in batch

Fig. 1 Photocatalytic mechanism using Yb-TiO₂-rGO photo catalyst [3]



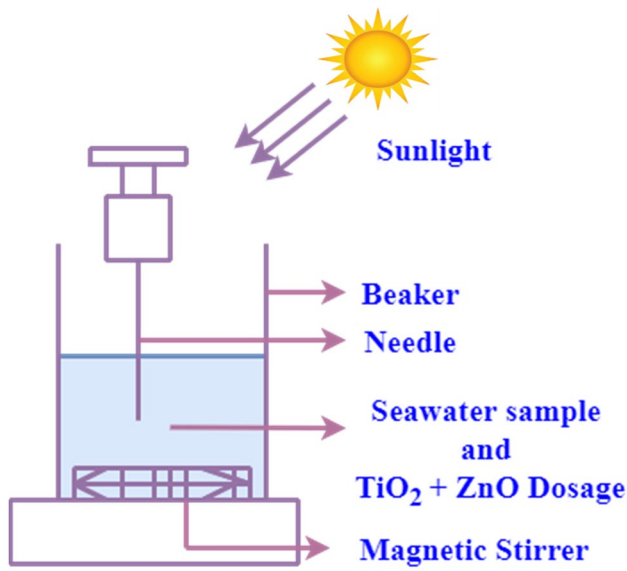


Fig. 2 The experimental setup of batch reactor

and continuous reactors using TiO_2 catalyst and natural solar energy. It was observed that substantial reduction in pollutants present in the oil produced water [7].

Nayeem et al. [8] presented a complete review on various photo catalytic studies involving seawater and saline industrial waste water including oil produced water. This review discusses theoretical and practical methods for the photocatalytic destruction of contaminants in saline water. The pipe, slurry and packed reactor systems were employed using TiO_2 photo catalyst for the removal of benzoic acid and phenol under the natural and artificial UV source. It was observed a significant removal of organic compounds within the study parameters [9]. The Nano TiO_2 photo catalyst was used in a batch reactor system to investigate the degradation of pollutants in saltwater such as bacteria, halogenated carbon, suspended solids, etc. A complete removal of bacteria and substantial reduction of other pollutants was reported in [10]. In order to photo catalytically degrade the inorganic carbon contained in seawater, TiO_2 was used in thin films and suspension mode with H_2O_2 . Stability in the coated film as well as a considerable decrease in inorganic carbon were seen [11].

The Response surface approach has been widely used to optimize experimental variables in order to identify the influence of independent factors on responses. To reduce the number of experiments, the Box Behnken tool were employed in RSM with the optimum response. It was observed that there is an optimal COD percentage removal with the concentration of pH. Artificial fiber networks are a sophisticated tool in MATLAB used to predict the experimental parameters. The tan sigmoid function with hidden layer and linear function were employed into three

parts. In ANN, the independent variables are taken into account as one hidden layer and output layer for the independent variables POME concentration, pressure, time, and pH. It observed that the ANN shows the predicted optimum values closed with the experimental results with high accuracy in the process of filtration [12]. Response surface approach and a genetic algorithm tool were used to undertake statistical modelling in order to obtain the desirability function and forecast values. It was observed that the RSM-GA predicted well with the experimental values [13]. A statistical model was developed with three independent variables using RSM (Design Expert) and ANN-LM. This model forecasts the values for the COD, TOC, BOD, and biodegradability removal efficiencies [14]. Under sun irradiation a UV lamp was employed to remediate contaminants in the petroleum effluent with a hematite catalyst. RSM modelling was performed for the statistical analysis. It was observed remarkable results with a good improvement in raising the biodegradability. The biodegradability enhanced from 0.074 to 0.604 with a duration time of 90 min. The COD removal was found to be 90.85% with a catalyst dosage of 5 g/L and pH 7.5 [15]. Srinivas et al., [16] studied ANN structure, training size, and transfer function were instantaneous and effectively generated using the innovative ANN design algorithm TRANSFORM. For a highly nonlinear continuous casting model of a steel facility that has been industrially tested, it was utilized to construct ANN substitutes. With the aid of ANN, the casting model underwent multi objective optimization to assure optimum productivity, greater energy savings, and minimal operational costs. Non-dominated Genetic Algorithms for Sorting. The artificial neural network GA and RSM were employed with five dependent variables such as combination of dosages like TiO_2 and Fe^{2+} , reaction time, pH, airflow rate. The variation coefficient, mean square error and mean error were evaluated under the maximum operating conditions.

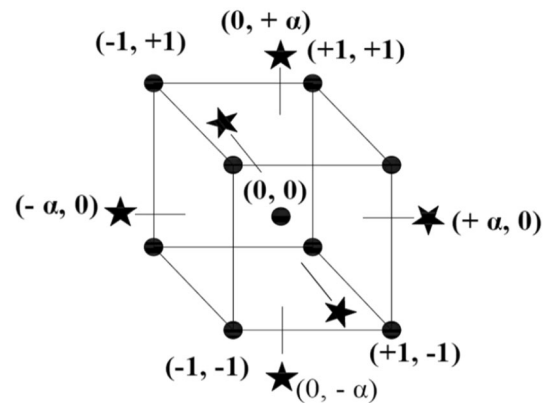


Fig. 3 Factors in the primary composite design [20]

The results found to be well predicted (67.2%) with artificial neural Network-Genetic Algorithm with experimental output (65.4%) for the removal of TOC [17].

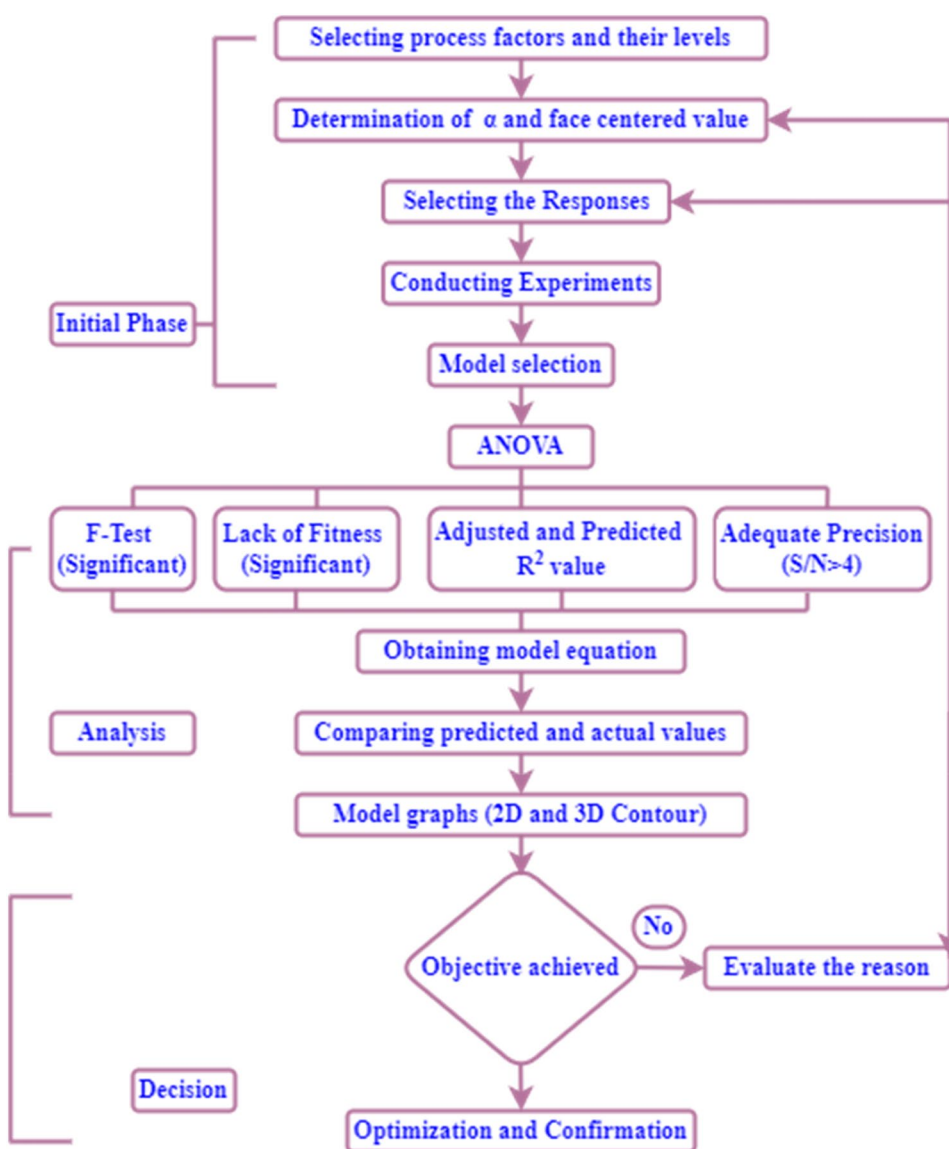
The ratio of BOD to COD is characterized as biodegradability, which is critical in the removal of contaminants from seawater. The performance of treatment technology depends upon the achievement of higher degree of biodegradability. Higher biodegradability in seawater indicates low fouling characteristics of the seawater. The biodegradability removal efficiency of seawater under the natural sunlight UV radiation with the combination of photo catalyst TiO₂ and ZnO is not reported in the literature. This study was conducted to optimize the experimental parameters using RSM and ANN statistical methods. A mixture of TiO₂ and ZnO was used to photo degrade pollutants in seawater and the performance was measured by

measuring the percentage elimination efficiencies of COD, TOC, BOD, and biodegradability.

Materials and Methods

A sample of saltwater measuring 5 L was taken at a depth of 10 m from the water’s surface at a location 2.3 km from the Khobar Beach in the Kingdom of Saudi Arabia. In this experiment, commercial TiO₂ Degussa P-25 (80% A-20%R) purchased from Evonik industries, Germany (99.9% purity) and ZnO obtained from mkNano, Canada (99.9% pure, APS: 20 nm) were employed as catalysts. COD was analyzed using an AQ 400, thermo scientific Orion COD 125 and total carbon analyzer (SHIMADZU). A pH meter (JENWAY 3520) was used to measure pH and a BOD incubator (Thermo

Fig. 4 Shows the systematic sequential procedure for the response surface method in which consisting of initial phase, analysis and final decision [22]



Fisher Scientific) with a complete set of water analysis kit (Eutech PCD 650) was utilized to estimate DO and BOD. Table 1 displays the original seawater parameters.

Experimental Study

Figure 2 displays a schematic of the experimental design of the batch experiments. A glass beaker of 1500 ml capacity with a magnetic stirrer was used as a batch reactor. The seawater sample of 1000 ml was taken in a batch reactor setup and the catalysts TiO₂ and ZnO was added. The photo catalytic process was conducted between 10:00 a.m. to 2:00 p.m. in the natural sunlight while being constantly stirred with a magnetic stirrer. The samples were taken out for analysis at equal intervals.

Equation 10 was used to estimate the percentage extraction efficiency of the observed values.

$$\text{Percentage removal} = \frac{(X_0 - X_f)}{X_0} \times 100 \tag{10}$$

where X₀ and X_f are the initial and final concentrations in mg/L respectively.

Mathematical Modelling Using RSM-CCD

The design expert application (version-11.1.2.0, Stat-Ease Inc. Minneapolis, MN, USA) was employed for the modelling, optimization of data and statistical design experimental runs. It is a commonly used and well-recognized statistical approach for experimental purposes used to assess the coefficients in mathematical models, anticipate the input factors influencing the reaction, and optimize output [18]. The best circumstances and the correlation between the intended result and unrelated input factors like dose, reaction time, and pH may be determined. It may be used to determine the best experimental parameter value for a maximum or lowest response value. In this study, the independent variables are changed in accordance with the

face-centered CCD at three levels, which are, respectively, -1 (low), 0 (the center point) and +1 (high). The adapted second-order polynomial regression model, also called the quadratic model, was used to suggest approximation [19]. The factorial points (-1, -1), (+1, -1), (-1, +1), and (+1, +1) are displayed in Fig. 3. The central points and axial or star points are (0, 0) and (-α, 0), (+α, 0), (0, -α) and (0, +α) in the central composite design [20].

The Eq. 11 can be used to understand the intended response and independent input variables as

$$y = f(x_1, x_2, x_3, x_4, \dots x_n) \pm \epsilon \tag{11}$$

where, y is the response, x_n is the variables and ε is the fitting error.

According to the central composite design (CCD), the experimental data and the ‘f’ were determined as an approximation. Equation 12 is the quadratic second-order polynomial regression model.

$$f = a_0 + \sum_{i=1}^n a_i x_i + \sum_{i=1}^n a_{ii} x_i^2 + \sum_{i=j}^n a_{ij} x_i x_j + \epsilon \tag{12}$$

where, a_i, represents the effect of x_i, a_{ii}, represents the effect of quadratic x_i, and a_{ij}, represents the linear interactions

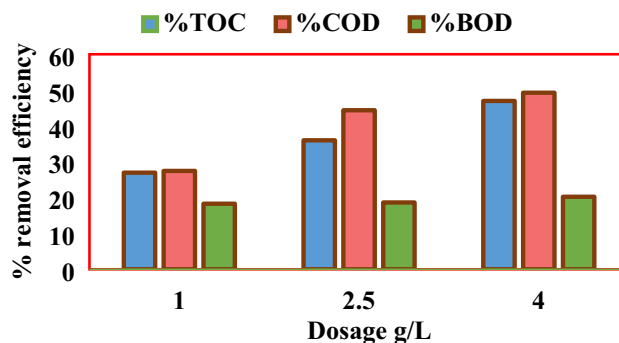
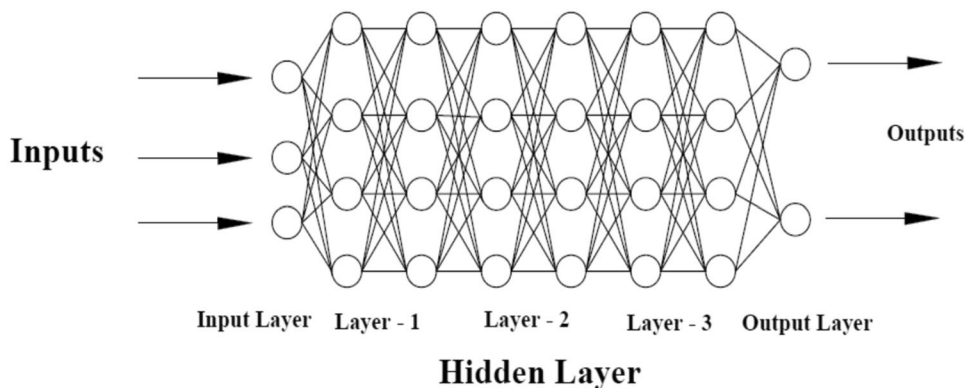


Fig. 6 % elimination effectiveness in relation to photo catalyst dose

Fig. 5 Architectural Neural Network with input and output variables [30]



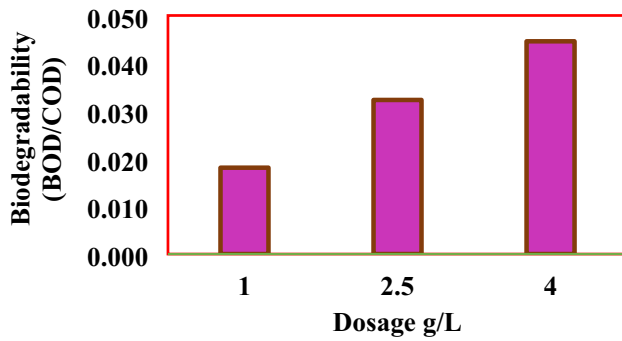


Fig. 7 Comparison of photo catalyst dose and biodegradability

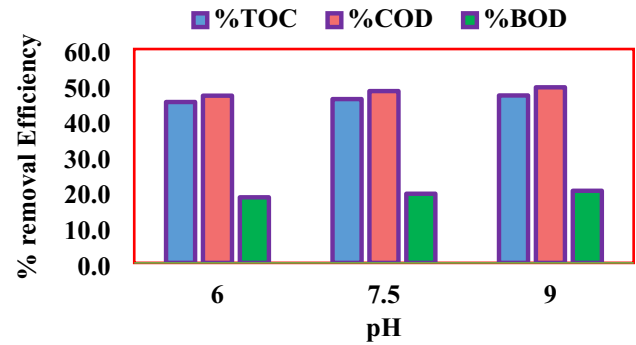


Fig. 10 Percent elimination rate against pH

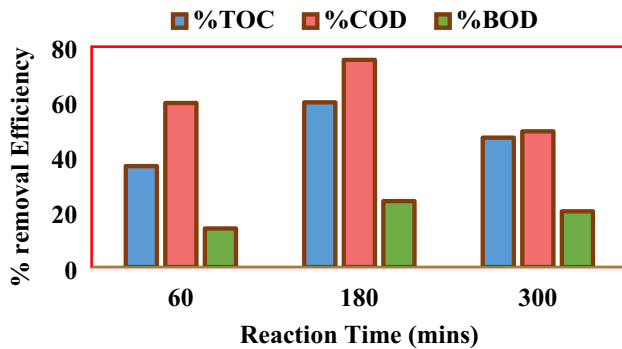


Fig. 8 Ratio of response time to removal efficiency

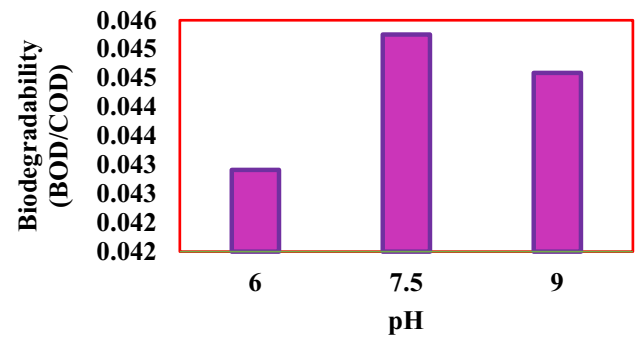


Fig. 11 Biodegradability versus pH

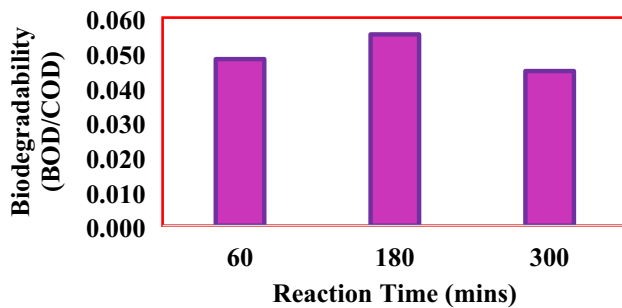


Fig. 9 Biodegradability versus reaction Time

- Selection of response percentage elimination of responses.
- Selection of variables and assigning the codes.
- Design and creation of experimental values for the elimination of replies by percentage.
- Performing regression analysis.
- Employing or formation of a quadratic polynomial according to the equation or response development.
- Developing the 2D and 3D contour plots and surface for the responses observed.
- Finally, performing analysis of optimum operating conditions, etc.

The sequential process of response surface method is summarized in Fig. 4.

Modelling Using ANN-Tool

The commercial Artificial Neural Network tool in MATLAB R2021b with Damped Least Squares (DLS) method or LMA Levenberg–Marquardt method was employed in the present study to optimize the input variables. To evaluate the data in this method, multilayer normal feed forward and full feed forward neural networks were used. The neural network, which is most frequently used to resolve engineering issues,

between x_i and x_j [21]. In order to determine the graphical analysis of the data and to ascertain how the independent variables and the answers interacted, the ANOVA (analysis of variance) method was used. The optimum region was achieved by the two and three-dimensional contour plots. In RSM, the process of optimization for the variables, factors and responses were comprising of different steps [22].

Table 2 Levels of experimental variables in the central composite design

Factor	Name	Units	Type	Min	Max	Coded low	Coded high	Mean	SD
<i>P</i>	<i>P</i> : Dosage	(g/L)	Numeric	1.00	4.00	-1 ↔ 1	+1 ↔ 4	2.50	1.19
<i>Q</i>	<i>Q</i> : Duration Time	(Min)	Numeric	60.0	300.0	-1 ↔ 60	+1 ↔ 300	180.0	94.87
<i>T</i>	<i>T</i> : pH		Numeric	6.0	9.00	-1 ↔ 6	+1 ↔ 9	7.50	1.19

Table 3 Results of an ANOVA for TOC removal

Source	Sum of Sqrs	DOF	Mean Sqr	<i>F</i> -value	<i>p</i> -value	
Model	3529.88	9	392.21	17.23	0.0006	Significant
<i>P</i> : Dosage	2111.63	1	2111.63	92.77	<0.0001	
<i>Q</i> : Reaction Time	751.08	1	751.08	33.00	0.0007	
<i>T</i> : pH	48.96	1	48.96	2.15	0.1859	
PQ	37.35	1	37.35	1.64	0.2410	
PT	2.62	1	2.62	0.1151	0.7443	
QT	0.1028	1	0.1028	0.0045	0.9483	
<i>P</i> ²	0.6766	1	0.6766	0.0297	0.8680	
<i>Q</i> ²	493.27	1	493.27	21.67	0.0023	
<i>T</i> ²	39.80	1	39.80	1.75	0.2276	
Residual	159.33	7	22.76			
Lack of fit	146.67	5	29.33	4.63	0.1871	Not significant
Pure er	12.67	2	6.33			
Cor total	3689.21	16				

Table 4 Results of an ANOVA for COD removal

Source	Sum of Sqrs	DOF	Mean Sqr	<i>F</i> -value	<i>p</i> -value	
Model	4896.07	9	544.01	149.66	<0.0001	Significant
<i>P</i> : Dosage	2665.93	1	2665.93	733.41	<0.0001	
<i>Q</i> : Reaction Time	0.2205	1	0.2205	0.0607	0.8125	
<i>T</i> : pH	55.69	1	55.69	15.32	0.0058	
PQ	155.64	1	155.64	42.82	0.0003	
PT	0.3886	1	0.3886	0.1069	0.7533	
QT	1.51	1	1.51	0.4150	0.5400	
<i>P</i> ²	113.49	1	113.49	31.22	0.0008	
<i>Q</i> ²	903.44	1	903.44	248.54	<0.0001	
<i>T</i> ²	0.6899	1	0.6899	0.1898	0.6762	
Residual	25.44	7	3.63			
Lack of fit	24.78	5	4.96	14.87	0.0642	Not significant
Pure error	0.6667	2	0.3333			
Cor total	4921.52	16				

uses feed forward with backward propagation. The number of neurons in architectural neural networks is comparable to that of the biological nervous system or brain of living things. ANN is a biological nervous system, which combines the processing layers with the help of simple elements in parallel operation. The neural network can be trained with different types of optimization function, for example Levenberg–Marquardt algorithm (LM), back and batch back propagation (IBP), (BBP) and Genetic Algorithm (GA) [23]. LM

optimization uses local search operation in contrast to GA providing and it has better efficiency compared to other gradient based algorithms [24]. Therefore, the proposed ANN is trained using the Levenberg–Marquardt algorithm (LM). The input layer, hidden layer (with one or more), and output layer makes up the architectural network. The independent variables of experimental data consist of input nodes and the dependent variables as output layer nodes. There are several nodes or neurons in each layer, the nodes in each neural

Table 5 Results of an ANOVA for BOD removal

Source	Sum of Sqrs	DOF	Mean Sqr	F-value	p-value	
Model	364.82	9	40.54	30.69	<0.0001	Significant
P: Dosage	38.33	1	38.33	29.02	0.0010	
Q: Reaction Time	130.71	1	130.71	98.95	<0.0001	
T: pH	36.31	1	36.31	27.48	0.0012	
PQ	0.8452	1	0.8452	0.6398	0.4501	
PT	1.05	1	1.05	0.7982	0.4013	
QT	0.2388	1	0.2388	0.1808	0.6835	
P ²	0.5255	1	0.5255	0.3979	0.5482	
Q ²	97.60	1	97.60	73.89	<0.0001	
T ²	1.22	1	1.22	0.9231	0.3687	
Residual	9.25	7	1.32			
Lack of fit	6.58	5	1.32	0.9870	0.5728	Not significant
Pure error	2.67	2	1.33			
Cor total	374.07	16				

Table 6 Results of an ANOVA for BOD/COD

Source	Sum of Sqrs	df	Mean Sqr	F-value	p-value	
Model	0.0021	9	0.0002	71.36	<0.0001	Significant
P: Dosage	0.0020	1	0.0020	616.83	<0.0001	
Q: Reaction time	8.842E-07	1	8.842E-07	0.2686	0.6203	
T: pH	7.866E-06	1	7.866E-06	2.39	0.1661	
PQ	5.379E-06	1	5.379E-06	1.63	0.2419	
PT	2.312E-06	1	2.312E-06	0.7021	0.4298	
QT	2.949E-07	1	2.949E-07	0.0896	0.7734	
P ²	8.905E-06	1	8.905E-06	2.70	0.1440	
Q ²	0.0001	1	0.0001	16.75	0.0046	
T ²	2.031E-07	1	2.031E-07	0.0617	0.8110	
Residual	0.0000	7	3.292E-06			
Lack of fit	0.0000	5	4.476E-06	13.43	0.0708	Not significant
Pure error	6.667E-07	2	3.333E-07			
Cor total	0.0021	16				

Table 7 Model metrics

Statistical conditions	Model's developed values			
	TOC removal	COD removal	BOD removal	BOD/COD removal
R ²	0.9568	0.9948	0.9753	0.9892
Adj. R ²	0.9013	0.9882	0.9435	0.9754
Pred. R ²	0.6786	0.9591	0.8397	0.9142
Adeq Prec	14.3485	39.5194	19.2939	24.7024
SD	4.77	1.91	1.15	0.0018

layer use the final outputs of all nodes in the previous layer as inputs [25]. In this current optimization method, a multi-layer neural network was utilized to train the data, where R was input elements, S was number of neurons and multiple artificial neural network was employed [26]. In this neural

tool, a numerous network was iteratively performed to establish the functions like sigmoid, linear, bipolar linear hyperbolic, threshold linear, tangent function. In order to make an accurate value prediction and compare it to the experimental values, training, validation, and testing were used.

Table 8 Equations for models using coded and real factors

Coded factors	Real factors
TOC removal (%) = +36.53 + 14.53 × P + 8.67 × Q + 2.21 × T - 2.16 × PQ - 0.5724 × PT - 0.1133 × QT + 0.5025 × P ² - 13.57 × Q ² + 3.85 × T ²	= +44.44650 + 12.63965 × P + 0.446172 × Q - 23.46982 × T - 0.012005 × PQ - 0.254386 × PT - 0.0000630 × QT + 0.223347 × P ² - 0.000942 × Q ² + 1.71295 × T ²
COD removal (%) = +61.30 + 16.33 × P - 0.1485 × Q + 2.36 × T - 4.41 × PQ - 0.2204 × PT - 0.4343 × QT - 6.51 × P ² - 18.36 × Q ² + 0.5074 × T ²	= -40.32312 + 30.49388 × P + 0.537194 × Q - 1.13054 × T - 0.024505 × PQ - 0.097955 × PT - 0.002413 × QT - 2.89265 × P ² - 0.001275 × Q ² + 0.225533 × T ²
BOD removal (%) = +20.18 + 1.96 × P + 3.62 × Q + 1.91 × T - 0.3250 × PQ - 0.3630 × PT - 0.1728 × QT + 0.4429 × P ² - 6.04 × Q ² - 0.6746 × T ²	= -32.38678 + 1.85611 × P + 0.192733 × Q + 6.34379 × T - 0.001806 × PQ - 0.161347 × PT - 0.000960 × QT + 0.196841 × P ² - 0.000419 × Q ² - 0.299826 × T ²
BOD/COD = +0.0346 + 0.0143 × P - 0.0003 × Q + 0.0009 × T - 0.0008 × PQ + 0.0005 × PT - 0.0002 × QT + 0.0018 × P ² - 0.0045 × Q ² - 0.0003 × T ²	= -0.004211 + 0.004477 × P + 0.000130 × Q + 0.002021 × T - 0.0000045528 × PQ + 0.0000239 × PT - 0.00000106657 × QT + 0.000810 × P ² - 0.000000315014 × Q ² - 0.000122 × T ²

P, Dosage; Q, Reaction time; T, pH

The training, validation and testing are performed by using a multilayer number of neurons as shown in Fig. 5. In this method, the function called sigmoid transfer has been employed to transfer the function of input and hidden layers [27]. The sigmoid function is able to transform any real number to one between 0 and 1. Sigmoid is the common choice when probabilistic approach is used for prediction because it combines nearly linear, curvilinear and almost constant behavior [28, 29]. The network architecture consisting of inputs are pH, reaction time, and catalyst dosage with the number of hidden layers and four output responses. For the training, testing, and validation, subsets of data made up of 70%, 15% and 15% of the total data were used. The number of hidden layers and nodes is decided based on the trial and error when choosing an architecture for your neural network. While performing the trial and error method, we need to add the layers and neurons to the network at random intervals and will take a lot of time to achieve it. The input and output of ANN were estimated as shown in Eq. 13 [30].

$$Y = f(x_1, x_2, x_3) \tag{13}$$

where, Y=output variables. x_1 is pH, x_2 is reaction time, x_3 is dosage.

Results and Discussion

For the experimental data, the Eq. 10 was employed to calculate the percentage removal efficiencies and estimated biodegradability.

Effect of Photo Catalysts Dosage

Figures 6 and 7 show that the highest percentage removal efficiency for COD, TOC, and BOD were 49.3, 47, and 20.2% at the total catalyst dose of 4 g/L and the maximum biodegradability (BOD/COD) as 0.045.

Effect of Reaction Time

The percentage elimination efficiencies of output variables are shown in Figs. 8 and 9 with reaction time and biodegradability. With a 180 min reaction period, the maximum percentage removal efficiency for TOC, COD, and BOD were discovered to be 59.79, 75.2, and 23.94%, respectively and 0.055 as maximum biodegradability with the duration time for 180 min.

Effect of pH

Figures 10 and 11 show the biodegradability with pH variation and the greatest percentage elimination efficiencies of output variables. At pH 9 the greatest removal efficiencies in percentage for TOC, COD, and BOD were 46.9, 49.3 and 20.23%, respectively. The biodegradability is unchanged at pH 7.5.

RSM-CCD Studies

A response surface methodology approach based on the CCD (central composite design) was utilized to investigate the combination of three factors (P: Dosage, Q: Reaction Time, T: pH). To analyze the experimental results, a statistical analysis of the square surface polynomial model was used by the central composite plane with 17 experiments under a randomized sub-type (Table 2).

Analysis of (ANOVA) variance results for the models of responses TOC, COD, BOD and BOD/COD are given in Tables 3, 4, 5, 6. The developed model “F-value” was found to be 17.23, 149.66, 30.69 and 71.36 for TOC, COD, BOD and BOD/COD depicting that all these models are statistically significant. Large ‘F’ values may occur due to noise and there is only 0.01% chance. P-values of “Prob>F” were observed to be less than 0.0500, which is indicating that all the models terms are found to be as significant. The model terms for all the responses P, Q, T, PQ, PT, QT, P², Q², T² are found to be significant, and the p-values are less than 0.001, demonstrating the level of significance for developing models. The P-values are not significant or insignificant if the values are greater than 0.10.

Table 7 shows the R² and predicted values found close to unity and smaller standard deviation values indicate good and better well predicting response of the model developed. A ratio greater than 4 is preferred for determining the signal to noise ratio using acceptable precision. For the percentage removal efficiencies, Table 8 displays the real factor and coded factor equations and Fig. 12a, b, c and d displays the linear graphs for the responses.

Statistical Model Analysis Versus 3-D Surface Plots

The 3-D surface plots of reaction time vs. dose for the percentage removal efficiencies of responses are shown in Fig. 13a, b, c and d. The ideal or maximum catalyst dosage for the combination of TiO₂ and ZnO dosage is 4 g/L, 180 min of reaction time, pH 7.5, TOC 52%, COD 71.12%, BOD 23% and BOD/COD 0.0506 respectively. The model optimization of the chosen solution is depicted in Fig. 14 as ramps with a maximum desirability of less than 1.0.

The statistical model yielded a total of 70 solutions, with the best biodegradability selected at a dose of 4 g/L and a reaction time of 0.052 s at 162.748 min.

Levenberg–Marquardt Approach Investigations of ANN Modelling

A Neural Network tool in MATLAB R2021A was employed and the model was generated by utilizing the 3 inputs such as, dosage TiO₂ and ZnO (g/L), reaction time in min and pH. In ANN, hidden layers help separating non-linear data. Normal hypothesis suggests that for a small size dataset, few numbers of hidden layers are required. Thus a trial–error method was used analyzing the accuracy of the network to determine the hidden layers and number of neurons in each layer. The model was trained, validated and tested with a multilayer neural network architecture feed forward with back propagation with 3 inputs, 3 hidden layers and 4 output responses as shown in Fig. 15.

One of the ANN drawbacks of ANN configuration is its overfitting. The overfitting of ANN generates high training accuracy and low validation accuracy. The Fig. 16 analyse MSE over the epochs. It shows that there is no significant change in test curve before the validation curve. Therefore, there is least chance of overfitting. In the default setup of MATLAB, the training stops after six consecutive increases in validation error, and the best performance is taken from the epoch with the lowest validation error. The best performance is achieved at epoch 8.

The prediction accuracy of the neural network was used to calculate the correlation coefficient (R²) between regression analysis and root mean-square error (RMSE). The RMSE and R² were measured by the Eq. 14 and 15.

$$\text{RMSE} = \sqrt{\frac{1}{n} \sum (X_{\text{meas}} - X_{\text{est}})^2} \quad (14)$$

$$R^2 = \left\{ \frac{n \sum X_{\text{meas}} X_{\text{est}} - \sum X_{\text{meas}} \sum X_{\text{est}}}{\sqrt{[N \sum X_{\text{meas}}^2 - (\sum X_{\text{meas}})^2][N \sum X_{\text{est}}^2 - (\sum X_{\text{est}})^2]}} \right\} \quad (15)$$

where, RMSE and R² ranges in between –1 and +1 and N are the number of operating points and X_{meas} and X_{est} are used as measured and estimated variables. If it is close to a negative value, it indicates as a stronger negative linear relationship and positive value it indicates as a strong positive linear relationship. Figure 17 shows the maximum correlation coefficient values according to the training, testing and validation with a standard angle as 45° line linear. All of the points are situated extremely close to the straight line,

Table 9 Shows the experimental, RSM and ANN values

Input variables			TOC removal (%)				COD removal (%)				BOD removal (%)				BOD/COD			
No. of run	P: Dos. g/L	Q: R.T. (mins)	T: pH	Expt values	RSM Pred. Values	ANN Pred. Values	Expt values	RSM Pred. Values	ANN Pred. Values	Expt values	RSM Pred. Values	ANN Pred. values	Expt values	RSM Predicted Values	ANN Predicted values	Expt values	RSM Predicted Values	ANN Predicted values
1	1	180	7.5	15.5	22.5	15.404	35.555	38.46	35.555	18.962	18.66	16.685	0.0199	0.0221	0.0205			
2	4	300	6	45.14	46.83	48.006	46.915	47	46.915	18.399	17.79	18.726	0.0429	0.0435	0.0430			
3	2.5	300	7.5	34.67	31.63	34.782	42.605	42.79	42.605	17.036	17.75	17.090	0.0311	0.0297	0.0308			
4	2.5	180	7.5	35	36.53	36.960	61	61.3	61.173	19	20.18	21.414	0.035	0.0346	0.0340			
5	4	300	9	46.98	49.88	47.054	49.264	50.41	49.264	20.233	20.53	20.247	0.0446	0.0459	0.0452			
6	1	60	6	2.395	0.93	2.944	14.61	13.33	14.610	5.6705	5.57	5.733	0.0175	0.0163	0.0199			
7	2.5	180	9	43.17	42.6	43.290	65.491	64.16	65.491	22.478	21.41	22.412	0.0365	0.0352	0.0376			
8	2.5	180	6	35.89	38.17	40.168	57.564	59.44	57.564	17.285	17.6	17.227	0.0324	0.0334	0.0315			
9	1	300	9	26.96	26.29	27.036	27.446	27.01	27.445	18.292	17.99	18.950	0.0181	0.018	0.0205			
10	1	300	6	21.83	20.94	21.926	23.695	22.72	23.695	13.887	13.79	14.140	0.0181	0.0177	0.0193			
11	4	60	9	36.64	37.1	37.844	59.559	60.39	59.559	14.007	14.29	13.951	0.048	0.0486	0.0481			
12	2.5	180	7.5	38	36.53	36.960	62	61.3	61.173	21	20.18	21.414	0.034	0.0346	0.0340			
13	1	60	9	6.972	4.86	6.986	19.577	19.36	19.577	9.6477	10.45	9.764	0.0178	0.0173	0.0194			
14	2.5	180	7.5	40	36.53	36.960	62	61.3	61.173	19	20.18	21.414	0.034	0.0346	0.0340			
15	2.5	60	7.5	9.55	14.3	9.202	42.709	43.08	42.709	12.005	10.52	11.978	0.0293	0.0303	0.0286			
16	4	60	6	33.34	33.59	38.150	54.953	55.25	54.953	10.363	10.86	10.399	0.0451	0.0453	0.0453			
17	4	180	7.5	56.86	51.56	56.792	73.468	71.12	73.468	23.036	22.58	23.479	0.0533	0.0506	0.0512			

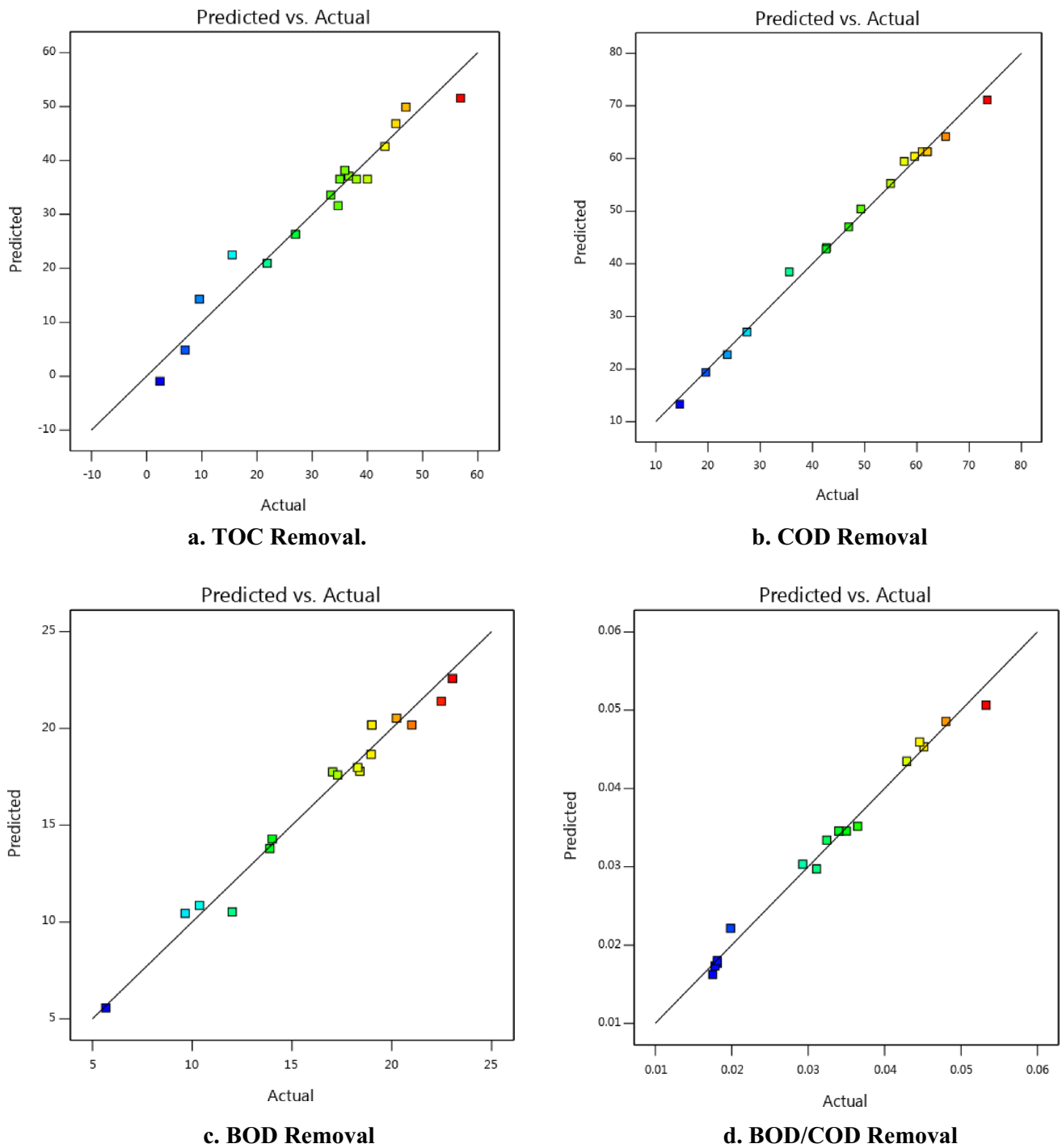


Fig. 12 RSM model linear plots for all responses

proving that the prediction made by the artificial neural network is accurate and outstanding within the legal area. For all response variables, the coefficient adjusted is very nearly

equal to unity ($R^2_{adj} = 0.99$) demonstrating accurate prediction. The coefficient of multiple determination is almost equal to unity ($R^2 = 1$), which is good and flawless.

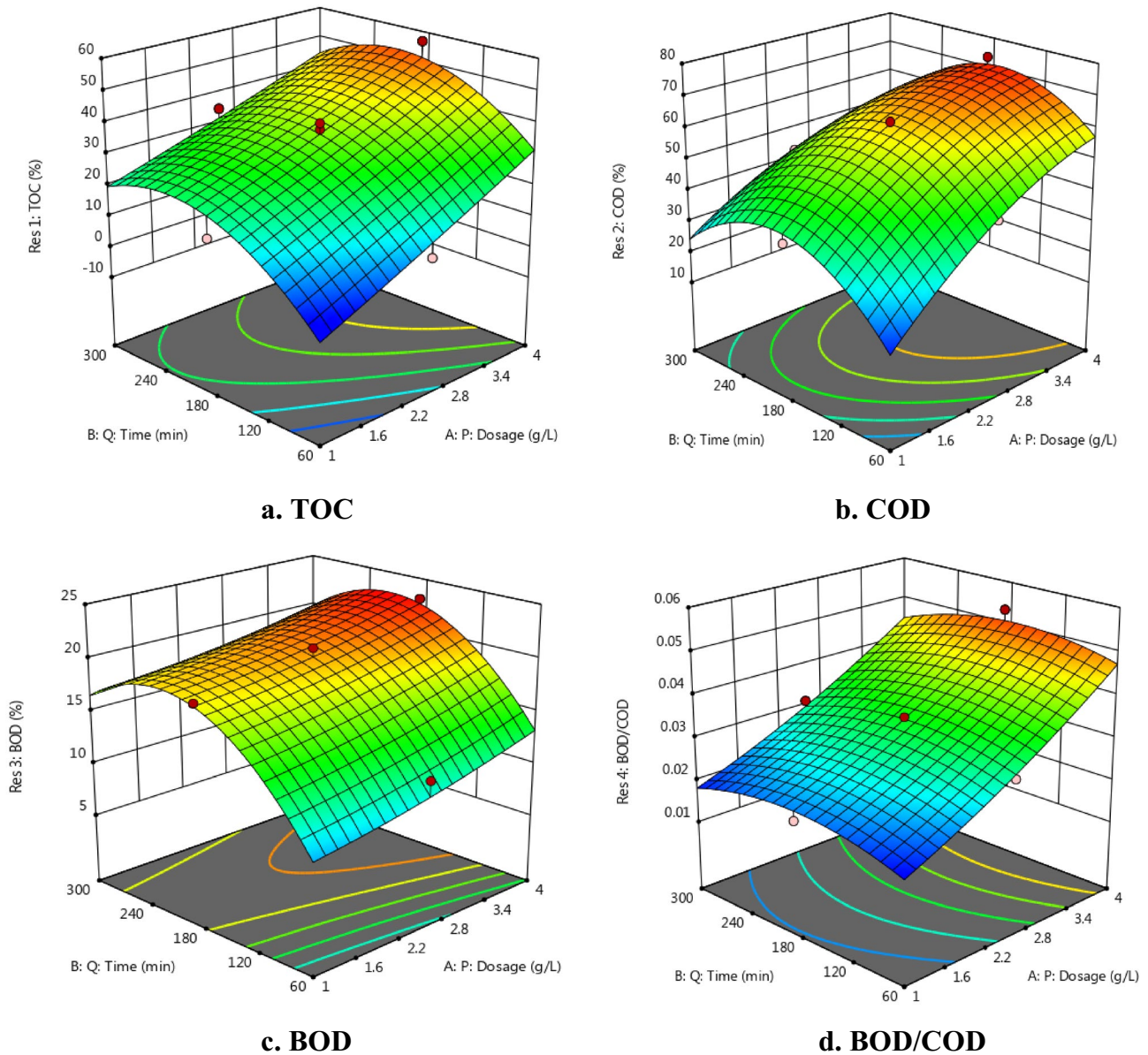


Fig. 13 (a, b, c and d) 3-D surface plot for all the responses

Statistical Model Comparison Between RSM-CCD and ANN-Tool

Based on the predicted inaccuracies, the Artificial Neural Network tool and Response Surface Methodology-Central Composite Design on predictive models for the percentage elimination efficiencies of TOC, COD, BOD, and biodegradability were compared with the experimental values. When comparing the RSM-CCD design of the ANN predictive model, the variance in predictive values for all response components was found to be greater. Table 9 shows the deviation of the values for experimental, RSM design and ANN. The comparison of the values of all response factors

is based on the quadratic model in RSM and training, testing, validation with a number of trails by ANN using the multilayer neurons. The ANOVA analysis from Tables 3, 4, 5 suggests that the p -value of lack-of-fit is not significant, i.e. p -value > 0.05, which indicates lack of evidence in the RSM regression model. Table 3 shows that there are 18.71% chances that a large error can occur due to noise. And therefore, there is a need to test another alternative. In this paper, ANN is used as an alternative to the RSM. RSM is classical statistical modelling. In contrast, ANNs can learn and simulate complicated, non-linear relationships. Thus ANN is able to recognize important relationship whereas RSM ignored it. Therefore, ANN gives better results than RSM.

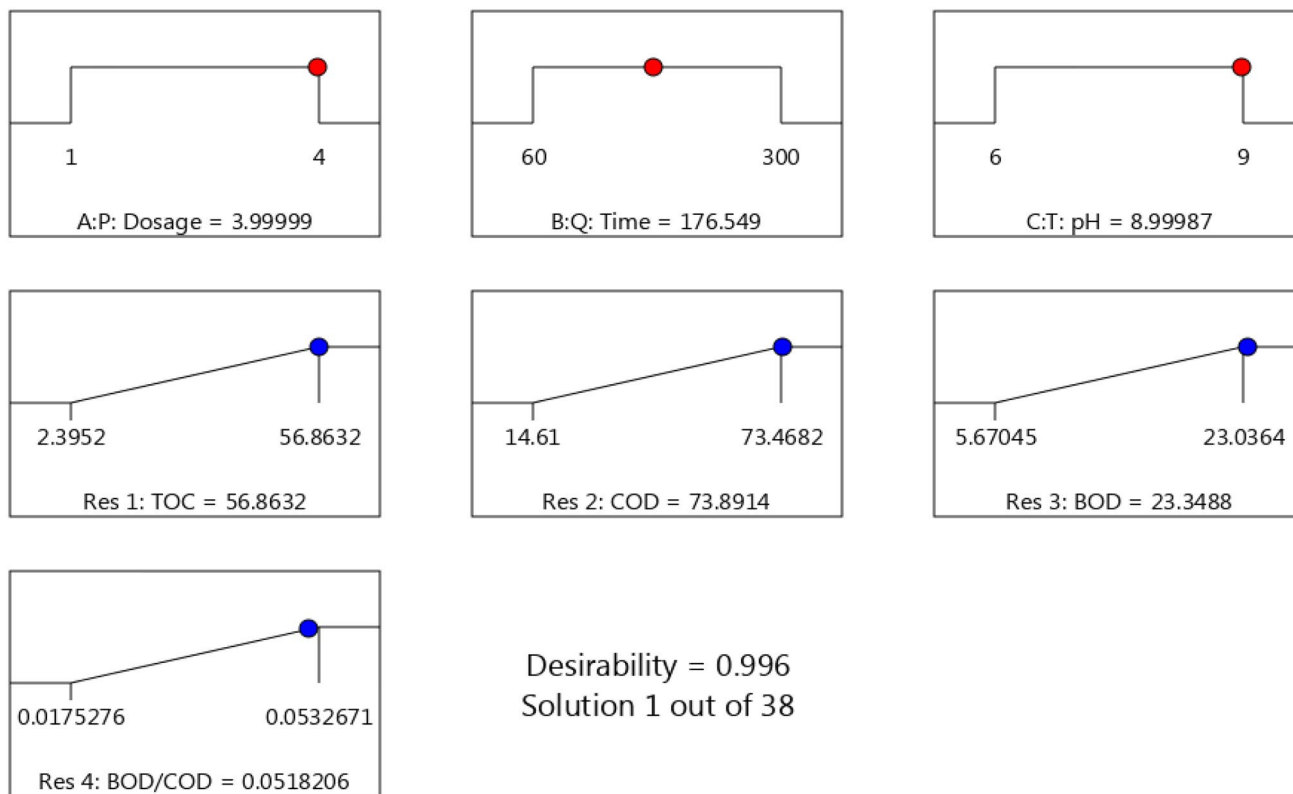


Fig. 14 Optimization ramps for the desirability of selected solution

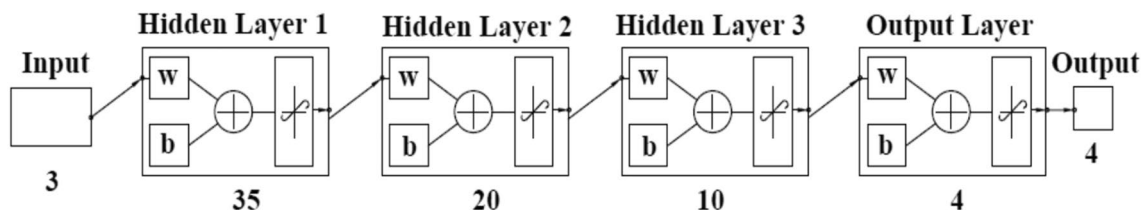


Fig. 15 Neural Network Feed-forward with back propagation

Conclusion

Under natural sun illumination, the elimination of contaminants found in saltwater was accomplished using a mixture of TiO₂ and ZnO photo catalysts. It was discovered that the seawater had significantly removed contaminants. The following are the conclusions drawn from the study:

- The highest experimentally determined percentage elimination efficiencies for TOC, COD, BOD, and biodegradability as 0.0533 were 56.9, 73.5, and 23.0%, respectively.
- The connection between the independent variables and responses was found to be accurately and suitably

described by a quadratic model. The P-value, F-value, and lack of fit test all confirmed the relevance of the RSM model. The maximum percentage removal efficiencies were found to be 56.9, 73.5 and 23.0% for TOC, COD, BOD and biodegradability as 0.0533.

- Based on optimization criteria, a total of 70 solutions were obtained using RSM-CCD statistical modelling, and all of the responses and factors had maximum desirability values that were less than 1.0. The optimal values of biodegradability at a dosage of 4 g/L (TiO₂ and ZnO) and at a reaction time of 163 min was found to be 0.052.
- According to RSM-CCD and ANN models, the optimal prediction values for the percentage elimination

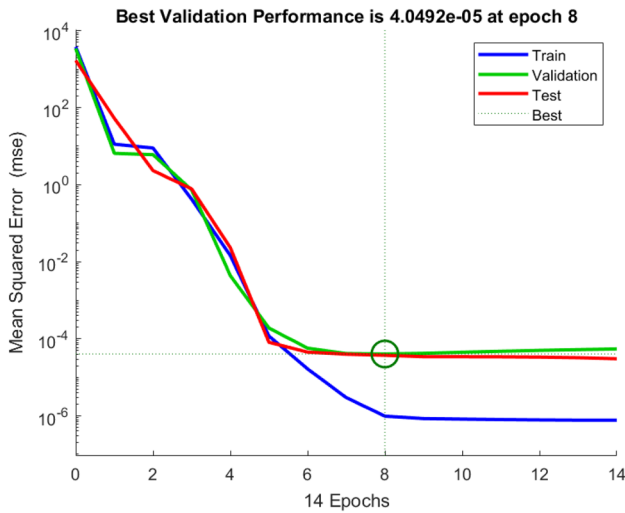


Fig. 16 MSE vs Epochs

efficiencies of TOC, COD, BOD and biodegradability were found to be 51.6, 56.8; 71.1, 73.5; 22.6, 23.5% and 0.0506, 0.0512 respectively at a photocatalyst dosage of 4 g/L for the reaction time 180 min and pH 7.5.

- By comparing the error functions and performing a linear regression analysis, the ANN and RSM-CCD models were compared. The projected values of the RSM-CCD and ANN statistical models were well associated with the experimental data. The RSM-CCD modeling’s average $R^2 = 0.8479$ was found to be inferior than the ANN model’s average $R^2 = 0.999$ for projected values. This clearly shows that the ANN model’s forecast was determined to be superior than the RSM-CCD model’s. The study also indicated that the artificial neural network may be a useful tool and a reliable substitute for the RSM-CCD model.

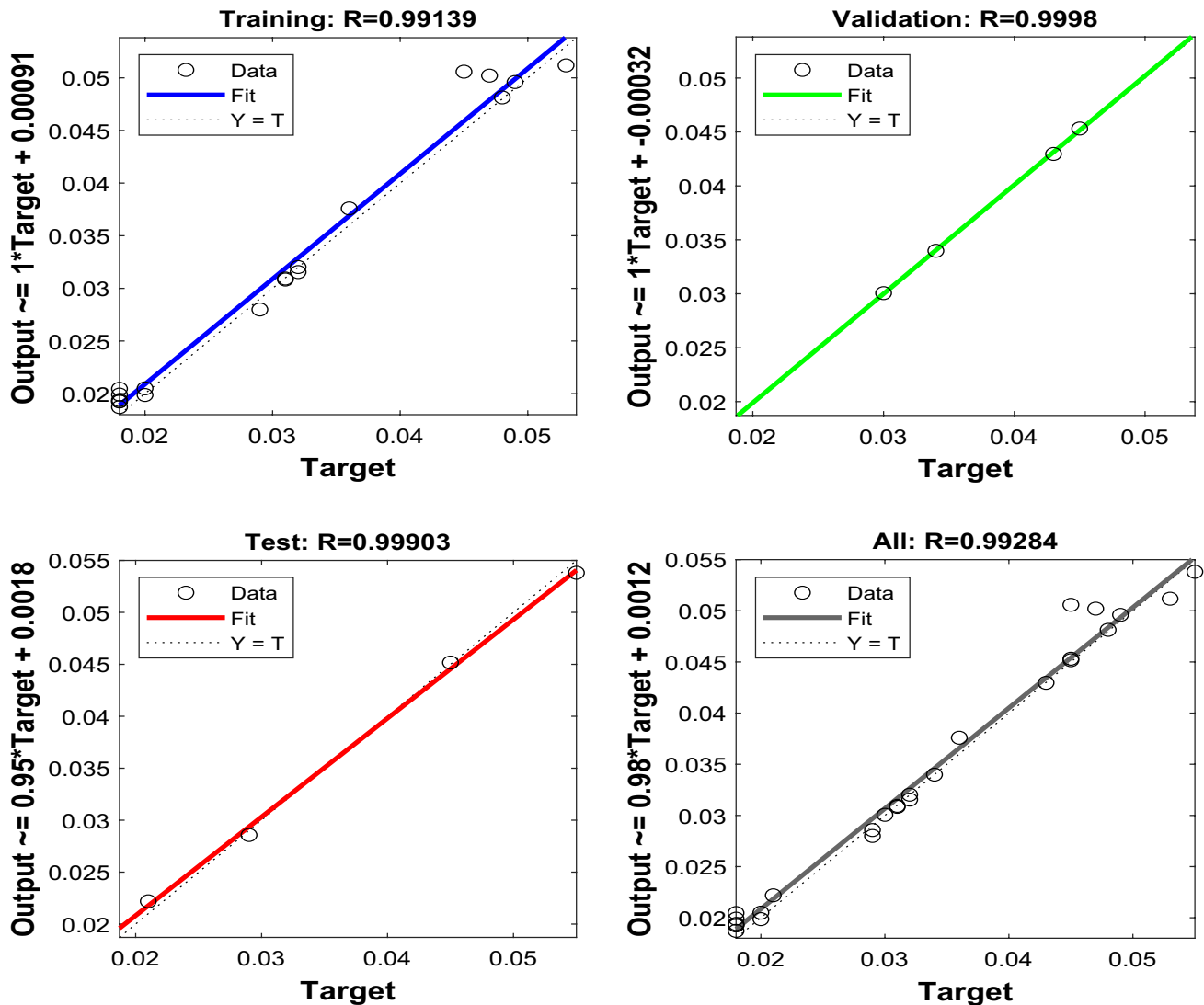


Fig. 17 Percentage removal efficiency according to ANN regression plots

Funding The authors for this research received no funding specific grant from any funding agency, etc.

Declarations

Conflict of interest The authors do not have any conflict of interest.

References

- H.A. Jabri, S. Feroz, Effect of combining TiO₂ and ZnO in the pretreatment of seawater reverse osmosis process. *Int. J. Environ. Sci. Dev.*, **6**(5), 348–351 (2015). <https://doi.org/10.7763/IJESD.2015.V6.616>.
- S. Feroz, M.S. Baawain, S. Saadi, M.J. Varghese, Experimental studies for treatment of seawater in a re-circulation batch reactor using TiO₂ P₂₅ and Polyamide. *Int. J. App. Eng. Res.* **10**(10), 26259–26266 (2015)
- H. Xu, Z. Hao, W. Feng, T. Wang, Y. Li, Mechanism of photo degradation of organic pollutants in seawater by TiO₂—based photocatalysts and improvement in their performance. *Am. Chem. Soc.* **6**(45), 30698–30707 (2021). <https://doi.org/10.1022/acsomega.1c04604>
- S. Feroz, N. Raut, R.A. Maimani, Utilization of solar energy in degrading organic pollutant-case study. *Int. J. COMADEM.* **14**(3), 33–37 (2011)
- E.B. Azevedo, A.R. Torres, F.R.A. Neto, M. Dezotti, TiO₂ – photo catalyzed degradation of phenol in saline media in an annular reactor: hydrodynamics, lumped kinetics, intermediates and acute toxicity. *Braz. J. Chem. Eng.*, **26**(1), 75–87 (2009). <https://doi.org/10.1590/S0104-66322009000100008>
- J. Qiuyi, Y. Xiaocai, Z. Jian, Q. Xinyang, Photocatalytic degradation of diesel pollutants in seawater by using ZrO₂ (Er₃₊)/TiO₂ under visible light. *J. Environ. Chem. Eng.* **5**(2) (2017). <https://doi.org/10.1016/j.jece.2017.01.011>
- M.A. Mashari, M.J. Varghese, S. Feroz, L.N. Rao Characterization and photocatalytic treatment of oil produced water-using TiO₂. *Int. J. Appl. Nanotechnol.*, **3**(1) (2016)
- M. Nayeemuddin, P. Palaniandy, S. Feroz, Pollutants removal from saline water by solar photocatalysis: a review of experimental and theoretical approaches. *Int. J. Environ. Anal. Chem.* (2021). <https://doi.org/10.1080/03067319>
- S. Feroz, A. Jesil, Treatment of organic pollutants by heterogeneous photocatalysis. *J. Inst. Eng. (India) Ser. E.* **1**, 45–48 (2012). <https://doi.org/10.1007/240034-012-0001-6>
- S. Feroz, F.A. Siyabi, Joefel, S. Saadi, Application of solar nano photocatalysis in treatment of seawater. *Int. Sci. J. Arch. Eng.* **3**(1) (2014)
- H. Jabri, A. Hudaifi, S. Feroz, F.A. Marikar, M. Baawain, Investigation on the effect of TiO₂ and H₂O₂ for the treatment of inorganic carbon present in seawater Res. Inventory. *Int. J. Eng. Sci.* **5**(2), 50–55 (2015)
- M. Said, M. Abbad, A.W. Mohammad, Optimization of palm oil mill effluent treatment by applying RSM and ANN. *Indonesia J. Fund. App. Chem.* **1**(1), 7–13 (2016). <https://doi.org/10.24845/ijfac.v1.i1.07>
- V.M. Joy, S. Feroz, S. Dutta, Solar nano photocatalytic pretreatment of seawater: process optimization and performance evaluation using response surface methodology and genetic algorithm. *App. Water Sci.* **11**(18) (2021). <https://doi.org/10.1007/s13201-020-01353-6>
- M. Nayeemuddin, P. Palaniandy, S. Feroz, Optimization of solar photocatalytic biodegradability of seawater using statistical modelling. *J. Indian Chem. Soc.* **98**(12) 2021 <https://doi.org/10.1016/j.jics.2021.100240>
- F.Y.M. Salih, K. Sakhile, F. Shaik N.L. Rao, Treatment of petroleum wastewater using synthesized haematite (α-Fe₂O₃) photocatalyst and optimization with response surface methodology. *Int. J. Environ. Anal. Chem.* (2020). <https://doi.org/10.1080/03067319.2020.1817422>
- S.S. Miriyala, V.R. Subramanian, K. Mitra, TRANSFORM-ANN for online optimization of complex industrial processes: casting process as case study. *Res.* **264**(1), 294–309 (2018). <https://doi.org/10.1016/j.ejor.2017.05.026>
- V.M. Joy, S. Feroz, Susmita D., TiO₂ / Photo-Fenton process for seawater pretreatment: modelling and optimization using response surface methodology (RSM) and artificial neural networks (ANN) coupled genetic algorithm (GA). *J. Indian Chem. Soc.* (2020) 10.5281/zenodo.5657210
- M.Y. Noordin, V.C. Venkatesh, S. Sharif, S. Elting, A. Abdullah, Application of response surface methodology in describing the performance of coated carbide tools when turning AISI 1045 steel. *J. of Mat. Proc. Tech.* **145**(1), 46–58 (2004). [https://doi.org/10.1016/S0924-0136\(03\)00861-6](https://doi.org/10.1016/S0924-0136(03)00861-6)
- S.J. Breig, K.J.K. Luti, Response surface methodology: A review on its application and challenges in microbial cultures. *Mat. Today. Proc.* **42**(5), 2214–7853 (2021). <https://doi.org/10.1016/j.matpr.2020.12.316>
- A.O Okewale, F. Omorowuo, O.A. Adesina, Comparative studies of response surface methodology (RSM) and predictive capacity of artificial neural network (ANN) on mild steel corrosion inhibition using water hyacinth as an inhibitor. *Inter. Con. Eng. Sust. World* **1378**, 022002 (2019) <https://doi.org/10.1088/1742-6596/1378/2/2022002>
- I.G. Ezemagu, M.I. Ejimofor, M.C. Menkit, O-Nwobi, Modelling and optimization of turbidity removal from produced water using response surface methodology and artificial neural network. *South Afr. J. Chem. Eng.*, **35**, 78–88 (2021). <https://doi.org/10.1016/j.sajee.2020.11.007>
- A.K. Gupta, P.S. Ghosal, S.K. Srivastava, Modelling and optimization of defluoridation by calcined Ca-Al-(NO₃)-LDH using response surface methodology and artificial neural network combined with experimental design. *J. Hazard. Toxic Radioact. Waste.* **21**(3) (2017) [https://doi.org/10.1061/\(ASCE\)HZ.2153-5515.0000343](https://doi.org/10.1061/(ASCE)HZ.2153-5515.0000343)
- M. Mourabet, A. Rhilassi, M. Ziatni, A. Taitai, Comparative study of artificial neural network and response surface methodology for modelling and optimization the adsorption capacity of fluoride onto apatitic tricalcium phosphate. *Uni. J. Appl. Math.* **2**(2), 84–91 (2014). <https://doi.org/10.13189/ujam.2014.020202>
- Prudencio, R. B., Ludermit, T. B., Neural network hybrid learning: genetic algorithms & Levenberg-Marquardt. In: *Between Data Science and Applied Data Analysis*, pp. 464–472, Springer, Berlin (2003)
- N.N. Desai, V.S. Soranganvi, V. K. Madabhavi, Solar photocatalytic degradation of organic contaminants in landfill leachate using TiO₂ nanoparticles by RSM and ANN. *Nat. Environ. Pol. Tech.* **19**(2). <https://doi.org/10.46488/NEPT.2020.v19i02.019> (2020)
- F.A. Ngwabebhoh, U. Yildiz, Pyrocatechol recovery from aqueous phase by nanocellulose-based platelet-shaped gels: response surface methodology and artificial neural network design study. *J. Environ. Eng.* **145**(2) (2019). 10.1061/(ASCE)EE.1943-7870.0001491
- S. Chamoli, ANN and RSM approach for modelling and optimization of designing parameters for a V down perforated baffle roughened rectangular channel. *Alex. Eng. J.* **54**(3), 429–446 (2015). <https://doi.org/10.1016/j.aej.2015.03.018>

28. T. Varol, A. Canakci, S. Ozsahin, Artificial neural network modeling to effect of reinforcement properties on the physical and mechanical properties of Al₂O₃–B₄C composites produced by powder metallurgy. *Compos. B Eng.* **54**, 224–233 (2013). <https://doi.org/10.1016/j.compositesb.2013.05.015>
29. Satyanarayana, G., Naidu, G.S., Babu, N.H., Artificial neural network and regression modelling to study the effect of reinforcement and deformation on volumetric wear of red mud nano particle reinforced aluminium matrix composites synthesized by stir casting. *boletín de la sociedad española de cerámica y vidrio*, **57**(3), 91–100 (2018). <https://doi.org/10.1016/j.bsecv.2017.09.006>
30. C.A. Igwegbe, O.D. Onukwuli, J.O. Ighalo, Bio-coagulation-flocculation (BCF) of municipal solid waste leachate using picralima

nitidaj extract: RSM and ANN modelling. *Current Res. Green Sust. Chem.*, **4** (2021). <https://doi.org/10.1016/j.crgse.2021.100078>

Publisher's Note Springer Nature remains neutral with regard to jurisdictional claims in published maps and institutional affiliations.

Springer Nature or its licensor (e.g. a society or other partner) holds exclusive rights to this article under a publishing agreement with the author(s) or other rightsholder(s); author self-archiving of the accepted manuscript version of this article is solely governed by the terms of such publishing agreement and applicable law.